Divalent Cation-Induced Lipid Mixing between Phosphatidylserine Liposomes Studied by Stopped-Flow Fluorescence Measurements: Effects of Temperature, Comparison of Barium and Calcium, and Perturbation by DPX†

Anne Walter*,‡ and David P. Siegel§

Department of Physiology and Biophysics, Wright State University, Dayton, Ohio 45435, and The Proctor and Gamble Company, Miami Valley Laboratories, P.O. Box 398707, Cincinnati, Ohio 45247

Received September 17, 1992; Revised Manuscript Received January 22, 1993

ABSTRACT: To understand the mechanism of membrane fusion, it is important to study the processes that mix the lipids of two apposed membranes. We measured the rates of divalent cation-induced aggregation and lipid mixing of bovine brain phosphatidylserine (BBPS) LUV, using light scattering and a resonance energy transfer assay. The lipid and divalent cation solutions were combined by stopped-flow mixing, which permitted measuring the half-times of aggregation and lipid mixing between pairs of liposomes. The collisional quencher DPX [*p*-xylenebis(pyridinium bromide)], used in a liposome contents-mixing assay, lowered the main transition temperature (T_m) of BBPS by about 10 °C and decreased the temperature threshold for lipid mixing. Since DPX was inside the liposomes for the latter measurements, this implies that perturbations to the inner monolayer affect the reactivity of the liposome. When palmitoyloleoyl-PS (POPS) was substituted for BBPS, little or no lipid mixing occurred. Ca^{2+}- and Ba^{2+}-induced BBPS aggregation and lipid mixing were compared as a function of temperature and divalent cation concentration. Aggregation rates were nearly insensitive to temperature and correlated with the percent of PS bound to either Ba^{2+} or Ca^{2+}. Above T_m, lipid-mixing rates increased with the Ba^{2+} and Ca^{2+} concentrations and temperature, even above the T_m of the Ba^{2+}/PS complex. Arrhenius plots were linear for both ions. The temperature dependence was greater for Ca^{2+}- than Ba^{2+}-induced reactions, and the slopes were independent of divalent cation concentration. When equivalent fractions of PS were bound with divalent cation at, and above, 20 °C, the lipid-mixing rate was greater with Ca^{2+} than with Ba^{2+}. The faster rate may reflect greater activation entropies and/or greater attempt frequencies at one or more steps in the Ca^{2+}-induced process. We conclude that stopped-flow mixing permits better characterization of initial interaction between liposomes, that small changes in the acyl chain region of the PS bilayer or the inner monolayer can have large effects on lipid-mixing rates, and that the differences between Ba^{2+}- and Ca^{2+}-induced interactions may be related to qualitative differences in the destabilization step.

Fusion between phospholipid membranes is an essential and ubiquitous biological process [e.g., Blumenthal (1987)]. In vivo fusion events are highly controlled in time and place, and although the regulatory pathways are being elucidated for a number of systems, the ultimate event, fusion between the membranes themselves, is not yet understood. Regardless of the control mechanisms or the presence of proteins potentially catalyzing biological fusion events, all fusion between membranes require that, at a discrete point, the membrane phospholipids rearrange to join the two bilayer membranes. The fusion event is likely to be fast [e.g., neurosecretion occurs in less than 1 ms after the electrical stimulus (Almers & Tse, 1990)]. A number of forces contributing to the stability and separation between the bilayers must be overcome. The identity of these forces and their relative contribution to the energetics of the fusion event have been surmised, but not demonstrated. In this study we reexamine one of the relatively simple model membrane systems in order to determine: (1) if measurements using stopped-flow mixing can be made at appropriate rates to determine the relevant time constants for aggregation and liposome defect formation rates and (2) if differences in the energy barriers of the rate-limiting steps for lipid mixing can be identified by comparing the temperature dependence of lipid mixing under different circumstances. The model system we have chosen is divalent cation-induced lipid mixing of large phosphatidylserine liposomes.

A number of technical and practical difficulties have hampered kinetic analysis of fusion in PS–divalent cation systems. First, the aggregation rates can be fast (milliseconds to seconds). This makes it difficult to measure aggregation rates accurately via hand-mixing experiments where the time necessary to completely mix the reactant solutions is about 1 s. Second, the nature of the liposome–liposome interactions changes qualitatively during the overall reaction. Initial events result primarily in fusion with the retention of aqueous contents, but the PS–divalent cation binding later results in strong adhesion between the membranes so that the liposomes collapse, leak their aqueous contents, and ultimately form multilamellar cochleate structures. In order to study the fusion process, data must be obtained as soon as possible after mixing, before a substantial fraction of the lipid in the system exists as large multilamellar aggregates. The comparatively long mixing times in hand-mixing experiments make it difficult to obtain data in this regime over a wide range of conditions.

The overall fusion or lipid mixing process can be divided into two discrete steps, aggregation and liposome destabili-

† This work was supported by ONR Contract No. N00014-88-K-0462.

‡ Wright State University.

§ The Proctor and Gamble Company.

0006-2960/93/0432-3271$04.00/0

zation, described by the following equations:

$$V + V \underset{k_{-1}}{\overset{k_1}{\leftrightarrow}} VV \xrightarrow{k_f} F \quad (1)$$

where V represents a single unilamellar liposome, VV a dimer aggregate, and F a fusion or lipid mixing product of two liposomes, k_1 and k_{-1} are the forward and reverse rate constants for aggregation, and k_f is the rate constant for the fusion or lipid-mixing step. In practice, k_f is essentially the rate of defect formation, since one criterion for experimental design is that the actual mixing and response of the components of the fluorescent assays occur faster than the fusion step itself. There may be multiple steps between aggregation and the final fusion product, but, for simplicity and lack of specific information, we are presently treating this as a single step.

Both aggregation and lipid-mixing rates will contribute to the overall rate of the reaction. The initial rate of aggregation is proportional to the square of the initial liposome concentration. The rate of defect formation is directly proportional to the concentration of dimer aggregates. At low initial liposome concentrations, the rate of dimer aggregate formation will be slow relative to defect formation, and the overall rate of fusion is controlled by the rate of aggregation. At high liposome concentrations, the rate of formation of dimer aggregates may be fast relative to defect formation rate so that the overall rate of fusion is controlled by the second step (k_f). The aggregation and fusion rates are independently susceptible to exogenous factors such as temperature so that the liposome concentrations at which one or the other process is predominant will vary with the experimental conditions. The kinetics of the fusion process have been described [for review, see Duzgunes and Bentz (1988) and Nir (1991)].

The stopped-flow technique simplifies the kinetic analysis and offers several other advantages over hand-mixing techniques. First, the excellent run-to-run reproducibility and ease of repetitive measurements allow data from many observations on the same sample to be averaged together. Therefore, reliable measurements can be made even in systems yielding very little fluorescence so that it is possible to get measurements that are well within the aggregation rate-limited regime. Second, the rapid mixing time (about 10 ms) allows accurate data recording at very short times after the overall reaction is initiated, i.e., the earliest phase of the overall reaction, which is the region that is informative about fusion events. Third, the rapid mixing time permits accurate measurements of the overall rate at very high lipid concentrations, where the time constants of the reactions can be as fast as tenths of a second, thereby permitting many systems to be in the defect formation rate-limited regime. The stopped-flow technique has the additional advantage that fusion is initiated by mixing of equal volumes of lipid suspension and divalent cation solution. In contrast, with hand-mixing experiments, a small volume of concentrated divalent cation or liposome suspension is mixed with a larger volume of the corresponding solution. This latter mixing protocol generates large local concentration gradients which, by nucleating aggregation and cochleate formation, result in qualitatively different phenomena that those observed at the final concentrations in the thoroughly mixed sample.

One reason for initiating the present study was to see if data obtained in the kinetic ranges made accessible by the stopped-flow technique changed any of the conclusions reached in prior extensive studies of this system [e.g., Wilschut et al. (1981, 1985), Ohki et al. (1982), Bentz et al. (1983), Nir et al. (1983), and Duzgunes et al. (1984)]. Our second goal was to use these methods to determine the temperature dependencies of the BBPS lipid-mixing rates induced by Ca^{2+} and Ba^{2+} as a means to investigate further the differences in the lipid-mixing rates observed for these two divalent cations. In the course of these studies, we found that encapsulated *p*-xylenebis(pyridinium bromide) (DPX)[1] alters the T_m and size as well as the aggregation and lipid-mixing rates of BBPS liposomes (the reason contents mixing was not included in this study). Liposomes formed from the defined lipid palmitoyloleoyl-PS (POPS) in contrast to BBPS did not exhibit lipid mixing despite extensive divalent cation-induced aggregation. Some of these data were presented in preliminary form (Walter et al., 1991).

MATERIALS AND METHODS

Chemicals and Buffers. Palmitoyloleoylphosphatidylserine (POPS), bovine brain phosphatidylserine (BBPS), and the headgroup-labeled lipids *N*-(7-nitro-2,1,3-benzoxadiazol-4-yl)phosphatidylethanolamine (NBD-PE) and *N*-(lissamine Rhodamine B sulfonyl)phosphatidylethanolamine (Rho-PE) were obtained from Avanti Polar Lipids, Inc. (Alabaster, AL) and were stored under nitrogen at −80 °C until use. DPX came from Molecular Probes (Eugene, OR). The salts were from Fisher Scientific, and the buffers HEPES [*N*-(2-hydroxyethyl)piperazine-*N*′-2-ethanesulfonic acid] and ethylenediaminetetraacetic acid (EDTA) were from Sigma Chemical Co. (St. Louis, MO).

The buffer solution was 100 mM NaCl, 10 mM HEPES, 0.1 mM EDTA, and 0.02% sodium azide titrated to pH 7.2 with NaOH prepared in twice-distilled water. Buffers for DSC and FTIR lacked sodium azide but were otherwise the same composition and were made up in distilled water processed by a Milli-Q system (Millipore Corp., Pleasanton, CA). The buffer was filtered through 0.2-μm filters and degassed prior to use. Divalent cation containing buffers were prepared from 1 M stock solutions of the chloride salt: actual concentrations of these stocks were confirmed by determining the chloride concentration (Chloridometer, Model 442500, Haake Buchler Instruments, Inc., Saddle Brook, NJ). The 90 mM DPX solution also contained 10 mM Na-HEPES (pH 7.2) and 0.1 mM EDTA.

Liposome Preparation. Liposomes were prepared by a combination of freeze–thaw and extrusion through 100-nm Nuclepore filters (Nuclepore Corp., Pleasanton, CA) in an Extruder (Lipex Biomembranes, Inc., Vancouver, BC, Canada) essentially following the method originally described (Hope et al., 1985). Lipid was deposited as a thin film on round-bottomed glass tubes by evaporating the chloroform solvent under a stream of nitrogen and was held in vacuo for at least 1 h. Buffer was added 1 h before subjecting the lipid to 10 freeze–thaw cycles. The lipid suspension was extruded under nitrogen 10 times at room temperature. Lipid concentrations were determined by measuring hydrolyzable phosphate (Ames & Dubin, 1960). The resulting liposomes

[1] Abbreviations: ANTS, 8-aminonaphthalene-1-3-6-trisulfonic acid; BBPS, bovine brain phosphatidylserine; DOPE-Me, monomethylated dioleoylphosphatidylethanolamine; DPX, *p*-xylenebis(pyridinium bromide); DSC, differential scanning calorimetry; EDTA, ethylenediaminetetraacetic acid; FTIR, Fourier-transform infrared; HEPES, *N*-(2-hydroxyethyl)piperazine-*N*′-2-ethanesulfonic acid; LUV, large unilamellar vesicle; NBD-PE, *N*-(7-nitro-2,1,3-benzoxadiazol-4-yl)phosphatidylethanolamine; POPS, palmitoyloleoylphosphatidylserine; Rho-PE, *N*-(lissamine Rhodamine B sulfonyl)phosphatidylethanolamine; SUV, small unilamellar vesicle; T_m, chain melting or $L_\beta \rightarrow L_\alpha$ phase transition temperature.

prepared from POPS or BBPS were primarily unilamellar, with a mean diameter of about 70 nm. Trapped volume was determined on several preparations by trapped 8-aminonaphthalene-1,3,6-trisulfonic acid (ANTS) and [^{14}C]mannitol, both indicating 1.4–1.8 mL/mol lipid. Average size and size distribution were monitored routinely by passing the liposomes over a high-performance gel filtration column TSK-G6000-PW (Beckman, Arlington Heights, IL) (Ollivon et al., 1986). The addition of NBD-PE and Rho-PE did not affect liposome size or size distribution. However, vesicles prepared with 90 mM DPX eluted later than control vesicles, indicating a smaller average diameter of about 60 nm (not shown).

Determination of T_m by Differential Scanning Calorimetry and FTIR. The lipid phase transition temperatures were monitored by differential scanning calorimetry (DSC) and, when necessary, by Fourier transform infrared (FTIR) spectroscopy. Samples were prepared from chloroform solutions of BBPS. The chloroform was removed by rotary evaporation and subsequent application of vacuum for 1 h at room temperature. For samples without divalent cations, the lipid film was hydrated with an appropriate amount of the corresponding buffer to produce a solution approximately 12.5 mg/mL in BBPS. The hydrated lipid was incubated on ice for 1 h or more and then subjected to five freeze–thaw cycles. The lipid suspension was then loaded into an MC-2 scanning calorimeter (Microcal Corp., Amherst, MA), equilibrated as close as possible to 0 °C, and a thermogram was obtained at a scan rate of 15 °C per hour. For thermograms obtained in the presence of Ba^{2+}, the dried lipid films were hydrated with the standard NaCl-HEPES buffer. After three freeze–thaw cycles, a stock solution of 1 M $BaCl_2$ in the same buffer was added to make the final solution 20 mM in Ba^{2+}. The sample was then frozen and thawed five additional times. This procedure ensured complete hydration and equilibration of the Ba^{2+} with the BBPS. For thermograms in the presence of Ca^{2+}, samples were treated as for the barium samples, except that the total concentration of Ca^{2+} was 15 mM.

The IR data were obtained with a Model FTS-40 FTIR spectrometer (Bio-Rad Laboratories, Richmond, CA) using a temperature-controlled, high-pressure, standard-size CIRCLE cylindrical internal reflectance cell (Spectra Tech, Inc., Stamford, CT) with a germanium internal reflectance element.

Aggregation and Lipid-Mixing Assays. To initiate aggregation and fusion, liposomes were combined with buffer containing the requisite divalent cation concentration by 1:1 volume mixing in a stopped-flow apparatus designed for fluorescence monitoring (Aminco-Morrow Stopped-Flow, SLM Instruments, Inc., Urbana, IL). The stopped-flow mixer was attached to a DMX-1000 fluorescence spectrometer with automatic data acquisition (SLM Instruments). The stopped-flow solution barrels and flow cell were thermostated by a circulating water bath. According the manufacturer's specifications, mixing was achieved in 5–10 ms: the time between data points for each experiment was always at least 50-fold shorter than the half-time for liposome dimer formation.

Aggregation was monitored by changes in intensity of the light scattered at 90° to the incident beam. Lipid mixing was followed by the change in fluorescence associated with decreasing energy transfer between NBD-PE and Rho-PE due to dilution of these fluorescent probes from labeled liposomes into unlabeled liposomes (Fung & Stryer, 1978; Duzgunes & Bentz, 1988). Excitation was at 470 nm and emission at 535 nm with 4-nm slits: a 515-nm long pass filter was placed in the emission path to minimize stray light contributions, especially due to scattering, to the signal. Control experiments indicated that stray light or scatter contributions to the fluorescent signal were generally undetectable. Appropriate corrections were made as part of the routine data analysis. For most experiments, the liposome population consisted of a 1:1 mixture of unlabeled liposomes and liposomes containing 0.7 mol % each NBD-PE and Rho-PE. The fluorescence expected for the transformation of all liposomes into fused dimers (hereafter referred to as "ideal dimer formation") was determined by running parallel experiments with liposomes prepared with 0.35 mol % of both fluorophores. Lipid-mixing rates are presented as the percent of ideal dimer formation per second and are corrected to account for the silent interactions. Identical rates were observed if the ratio of labeled to unlabeled liposomes was varied to 1:3 or 1:9, and the data were corrected for the probability of encounter.

The fluorescence data were calculated for presentation as the percentage of ideal dimer formation at a given time t using the paired "100% dimer" sample (liposomes with 0.35 mol % of both labels). The minimum fluorescence at $t = 0$ (F_0), taken as the average of the first three points, was subtracted from both samples, and the fluorescence of the lipid-mixing sample was divided by the fluorescence of the 100% dimer sample (F_{max_t}) at each time point:

$$\%\text{dimer formation}\ (t) = \frac{[F(1{:}1)_t - F_0]}{(F_{\max_t} - F_0)0.5}100 \qquad (2)$$

where $F(1{:}1)_t$ is the fluorescence observed during the lipid-mixing assay at time t, and the factor 0.5 represents the probability that the reacting pair of liposomes will be one labeled and one unlabeled. (When the initial ratio of labeled to unlabeled liposomes is 1:1, 50% of the initial interactions will result in no fluorescence change due to interactions between two labeled or two unlabeled liposomes.)

The liposomes did not shear in the stopped-flow apparatus as ascertained by the total lack of mixing-induced leakage (not shown). The progress curves were nearly identical with time in the mixing apparatus (i.e., the first curve was identical to the 10th or 20th repeat) which indicated that lipid was not precipitating in the flow cell or otherwise changing with time.

RESULTS

(1) Phase Transitions

(a) Mixtures of PS with Components of the Fluorescent Assay Systems. The temperature and width of the $L_\beta \rightarrow L_\alpha$ phase transition is characteristic for a particular lipid composition and can be perturbed by changes in the headgroup region (e.g., cation binding) or by the addition of other amphiphiles to the membrane. We determined T_m for each lot of PS. Different lots of BBPS have slightly different T_m values, which is not odd for a natural product. The values of T_m for the two lots of BBPS used in these studies were 6 and 9 °C (Figure 1). The values of T_m in two successive determinations for a given lot generally agreed within tenths of degrees. However, we did notice the T_m decreased by ca. 1.5 °C after storage of the unopened ampoules for a couple of months at −20 °C. (For lipid mixing studies, the lipid was stored at −80 °C.)

Thermograms were also obtained from mixtures of BBPS with the various probes used in the lipid-mixing assays to determine if the probes altered the transition position or width. The addition of NBD-PE and Rho-PE at 0.7 mol % had little or no effect on the transition (Figure 1a). However, when the

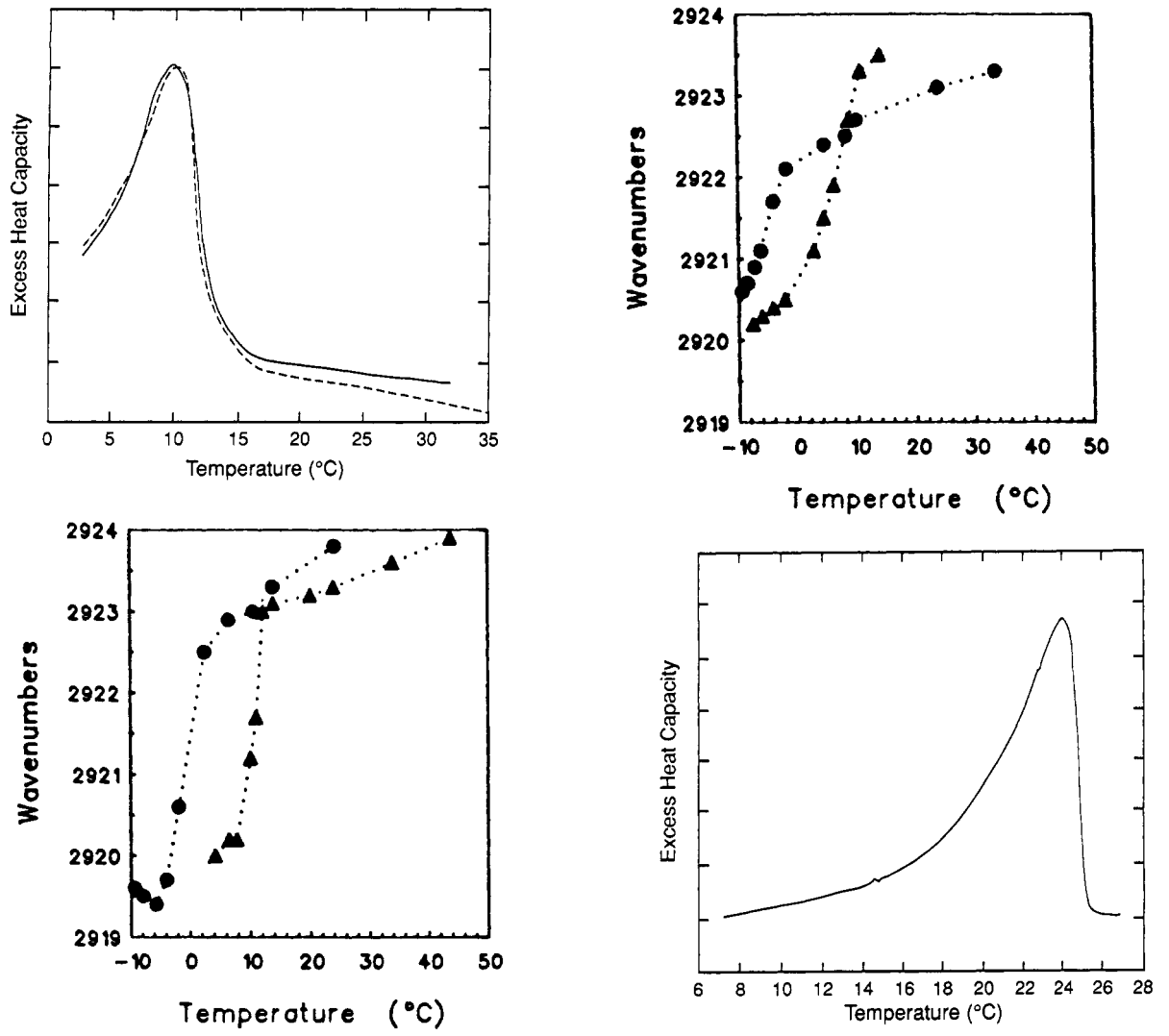

FIGURE 1: T_m determined by DSC and Fourier transform infrared (FTIR) spectroscopy for BBPS dispersed in the 0.1 M NaCl buffer under the various conditions tested in the aggregation and lipid-mixing experiments. (a, top left) Thermograms of BBPS alone (solid line) and BBPS with the fluorescent probes NBD-PE and Rho-PE incorporated at 0.7 mol % each (dashed line). (b, top right) FTIR determinations of the phase transition for BBPS with (circles) and without (triangles) 90 mM DPX. The plots are of the peak position of the CH_2 asymmetric stretch mode absorption peak in wavenumbers. (c, bottom left) FTIR determination of T_m for POPS (triangles) and POPS dispersed in 90 mM DPX buffer (circles) as a function of temperature. (d, bottom right) Thermogram of BBPS equilibrated with excess Ba^{2+}. The peak of the endotherm (T_m) occurs at 23.9 °C.

components of another commonly used fluorescent fusion assay, the ANTS/DPX contents mixing assay (Ellens et al., 1985), were tested, the collisional quencher DPX (at 90 mM, the concentration routinely used in fusion assays) appeared to abolish the transition as measured by DSC (not shown). When the DPX–BBPS samples were examined by FTIR using essentially the method of Casal et al. (1987), the transition was revealed to be 10 °C below the transition of the lipid in NaCl buffer; the same decrease in T_m was observed with DPX and POPS (Figure 1b,c). DPX is supplied as the bromide salt: an equivalent concentration of sodium bromide (180 mM) had no effect on T_m (not shown).[2] ANTS either had no effect or broadened the transition (not shown).

(*b*) *Divalent Cation-Induced* T_m. It is well known that titration of the PS headgroup by divalent cation binding will raise the transition temperature. In DOPS and POPS equilibrated with Ca^{2+}, the T_m is about 120 °C (Casal et al., 1987). The thermogram for Ba^{2+} and BBPS mixtures is shown (Figure 1d): the peak of the thermogram is 23.9 °C for the lot of BBPS used in most of these experiments. The transition in the presence of Ba^{2+} was clearly broadened and asymmetric. Thermograms with a similar shape and value for T_m (31.5 °C) were reported previously (Duzgunes et al., 1984). The difference in T_m may be ascribable to the variability in preparations of BBPS.

(2) Stopped-Flow Determination of Aggregation and Lipid-Mixing Rates

(*a*) *PS Concentration Dependence of Aggregation.* Aggregation was monitored by the initial changes in light scattering subsequent to mixing BBPS and divalent cation. An example of the light scattering curves observed as a function of increasing lipid concentration at constant divalent cation concentration (3.75 mM Ca^{2+}) and temperature (20 °C) is

[2] Despite a having a large effect on the T_m of PS, DPX did not significantly alter the $L_\alpha \rightarrow H_{II}$ phase transition temperature (T_H) of monomethylated dioleoylphosphatidylethanolamine (DOPE-Me) as determined by DSC (not shown). The T_H of DOPE-Me in the presence vs the absence of DPX was the same to within 0.7 °C in 20 mM $MgCl_2$ buffer at pH 9.9 and to within 0.5 °C in the absence of $MgCl_2$ at pH 7.4. DPX may not affect T_H in DOPE-Me because of the different nature of the $L_\alpha \rightarrow H_{II}$ transition or because of a low affinity of the DPX for DOPE-ME under these conditions. Therefore DPX probably does not perturb fusion kinetics in systems like DOPE-Me (Ellens et al., 1989).

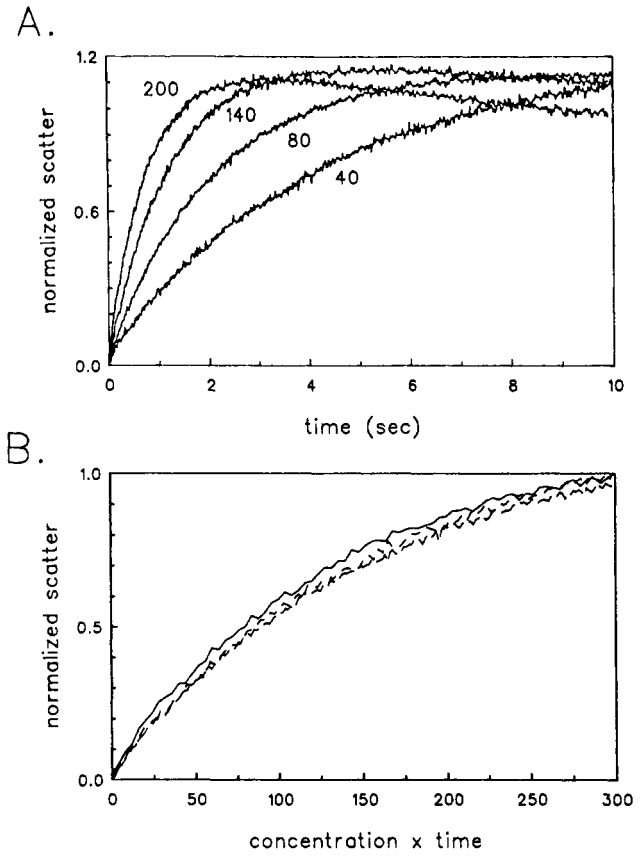

FIGURE 2: Changes in light scattering intensity represent aggregation. (A) the initial rise in scattered intensity as a function of BBPS concentration (3.75 mM Ca^{2+}, T = 20 °C). The scattered light intensity traces were normalized at the maximum scattered intensity for each lipid concentration, i.e., at 7.5, 3.75, 2.17, and 1.5 s, for 40, 80, 140, and 200 μM BBPS, respectively. Using the assumptions given in the text, the estimated rate constant for aggregation was calculated to be $(3.7 \pm 0.3) \times 10^8$ M^{-1} s^{-1}. (B) The data from panel a are plotted as a function of their respective lipid concentrations × time. These reduced plots are identical, as expected for a second-order process. Moreover, their identity indicates that the pathway followed during the initial stages of aggregation is independent of concentration.

given in Figure 2A. These curves have been normalized to the same initial and maximal values. No differences in light scattering vs time curves were observed among the various populations of liposomes tested, i.e., the fluorescently labeled liposomes and the unlabeled liposomes had identical scattering behavior.

The rate of rise in light scattering was shown to be a second-order process, as expected from the relationship stated in eq 1, by plotting the normalized data given in Figure 2A as scatter vs (μM PS)(time) (Figure 2B). The curves obtained at different PS concentrations overlaid one another, as would be expected for a second-order process. This result also indicates that the pathway for the initial aggregation events is the same for all PS concentrations tested (10–200 μM BBPS), meaning that qualitatively new types of aggregates did not form at higher lipid concentrations in this time regime.

Estimates of the aggregation rate could be obtained from the initial increase in the intensity of scattered light upon mixing divalent cations and PS liposomes. By comparing the rates of fluorescence dequenching and light scattering increase under clearly *aggregation-rate*-limiting conditions, it is clear that the rise in scattered light intensity to an initial plateau occurs at times very similar to those needed for ideal dimer formation. It is thus possible to estimate the aggregation rate constant. In this case (Figure 2), the rate constant for

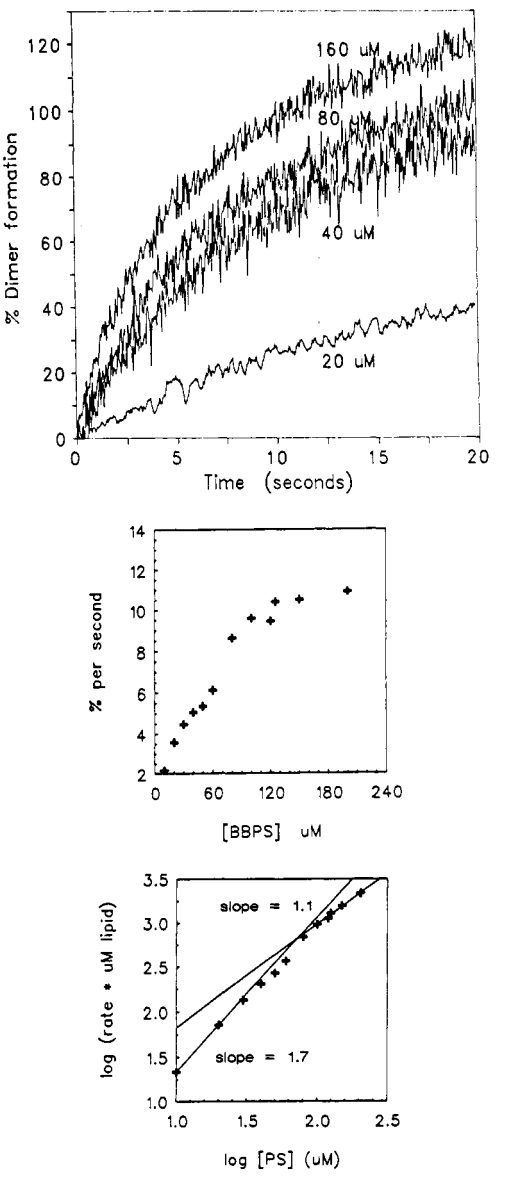

FIGURE 3: Lipid mixing followed by the change in energy transfer efficiency between the two fluorescent probes NBD-PE and Rho-PE as a function of total lipid concentration. (a, top) NBD-PE fluorescence was followed as a function of time after mixing the PS liposomes and divalent cation. The extent of lipid mixing was calculated from the percentage of the expected fluorescence expected if all the liposomes formed ideal reactive dimers. The examples shown are 20, 40, 80, and 160 μM BBPS, all in the presence of 3 mM Ca^{2+} at 40 °C. (b, middle) Lipid-mixing rates (%dimers/s) determined from the initial slopes (linear region taken at 20% or fewer dimers) of curves as shown in panel plotted as a function of total BBPS concentration (10–200 μM) (25 °C, 3 mM Ca^{2+}). (c, bottom) The data from panel b are plotted as rate × concentration vs concentration in a log–log plot to determine the apparent reaction order. The slope for lipid concentrations from 80 to 200 μM gives a slope of 1.1, which is close to 1 as required for a first-order reaction. The lipid concentration required to achieve first-order kinetics varies with temperature and divalent cation concentration.

aggregation was estimated to be 4×10^8 M^{-1} s^{-1} by assuming there are 5.5×10^4 lipids per liposome. Changes in light scattering beyond the initial plateau must be due to higher order aggregates, which may be new structures such as cochleate cylinders. Thus we can use the scattered light intensity traces as a guide for the rate of aggregation knowing that, in the time regime prior to the plateau, the mixture is still forming primarily dimeric aggregates.

(*b*) *PS Concentration Dependence of Lipid Mixing.* If the fusion or lipid-mixing step controlled the overall rate, it would

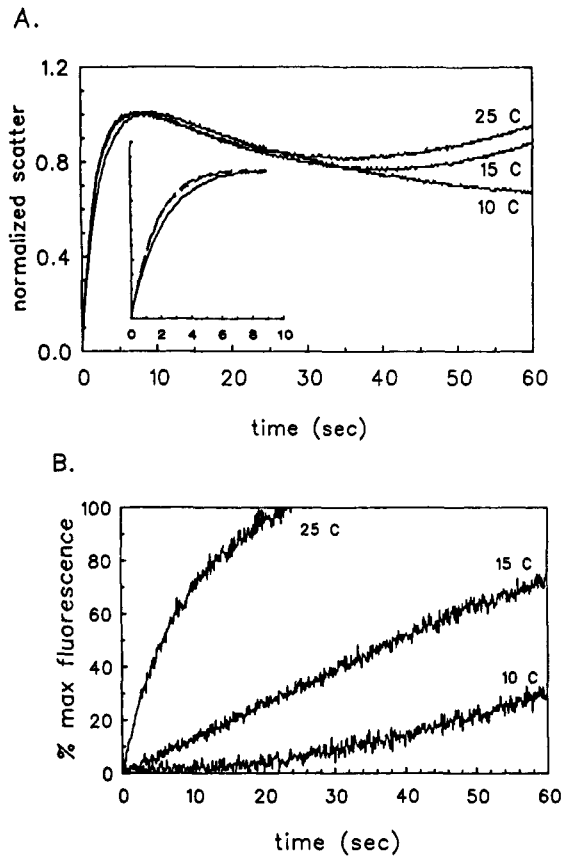

FIGURE 4: Effect of temperature on aggregation and lipid-mixing rates. (A) Changes in light scattering intensity were plotted as a function of time after BBPS was combined with Ca^{2+} to final concentrations of 100 μM and 3.75 mM, respectively, for samples at 10, 15, and 25 °C. The inset shows the same data over the first 10 s. (B) The change in NBD-PE fluorescence is plotted vs time for the same samples as in panel a.

make the rate appear first-order in lipid concentration (eq 1). In practice, the overall rate reflects the rates of both steps over a wide range of lipid concentrations. It is unlikely that the rate of the second step will ever *completely* control the overall rate, at least at experimentally feasible lipid concentrations. However, there are certainly conditions for which the primary influence on the overall rate is the rate of the second step, and the overall rate will approach first-order kinetics.

Lipid-mixing rates were determined from the first 20–30% of dimer formation/s from the data calculated as in eq 2. Examples of fluorescence changes with time are plotted in Figure 3a.[3] Lipid-mixing rates induced by 3 mM Ca^{2+} at 40 °C are plotted as a function of lipid concentration of Figure 3b, and a plot of the ln(rate·concentration) vs ln (concentration) is shown in Figure 3c. At low PS concentration (10–50 μM lipid), the lipid-mixing rate was almost second order in PS concentration (slope about 2), indicating that the rate of aggregation is rate-limiting. At concentrations above 80 μM, the observed overall rate was nearly first order in PS concentration (slope about 1), indicating that these lipid-mixing rates are in the regime where the rate of lipid defect formation, rather than aggregation, is rate-limiting. This is important, because it permits direct comparisons between the magnitudes of k_f as a function of changes in system composition and ambient conditions.

[3] Morris et al., (1985) observed a rapid transient in the NBD-PE fluorescence associated with the addition of Ca^{2+} that was not observed here. The difference may be due to the type of lipid used (PE vs PS) or the disposition of the fluorescent probes. Morris and colleagues combined NBD-PE labeled liposomes with Rho-PE labeled liposomes (probe mixing) so the initial fluorescence from the donor NBD-PE is high whereas, in the present study, the initial NBD-PE fluorescence was low due to efficient energy transfer to Rho-PE.

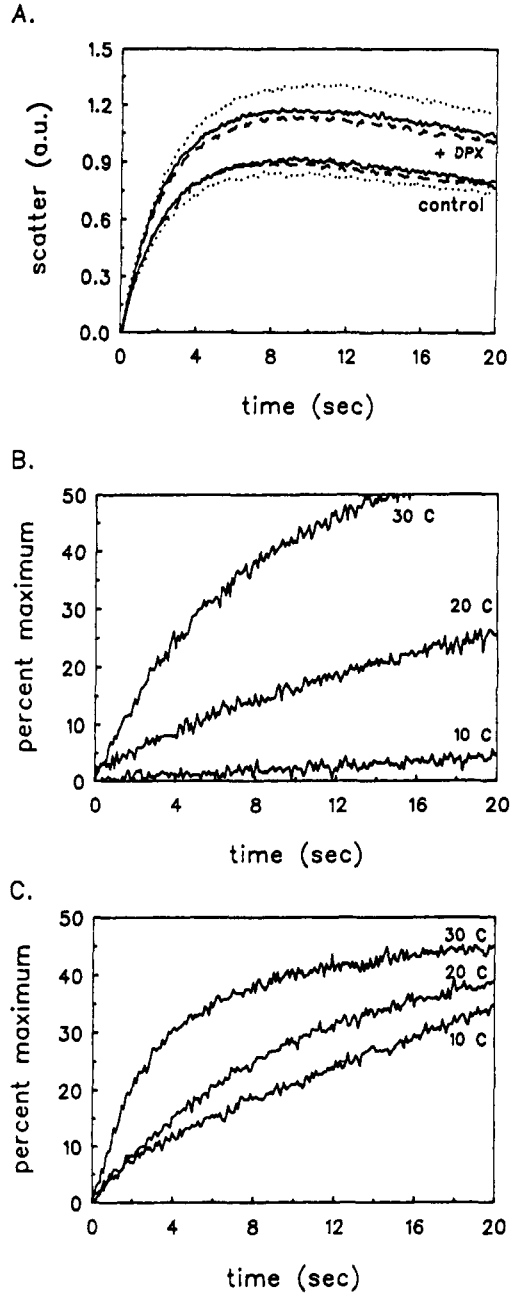

FIGURE 5: Effect of DPX on vesicle aggregation and lipid-mixing rates as a function of temperature in the presence of 3 mM Ca^{2+}. (A) The changes in scatter subsequent to stopped-flow mixing are plotted versus time for control and DPX-containing BBPS liposomes for three different temperatures (10, 20, and 30 °C are the solid, dashed, and dotted lines, respectively). Lipid-mixing rates are presented as percentage of the maximum NBD-PE fluorescence vs time for control (B) and DPX containing liposomes (C) at 10, 20, and 30 °C.

(3) Temperature Dependence of Aggregation and Lipid-Mixing Rates

Aggregation rates increased only very slightly with increased temperature (Figure 4A). The slight increase was less than is expected for the decrease in viscosity of the aqueous buffer as a function of temperature, suggesting that the process was not diffusion limited or that the rate of disaggregation increased

significantly with temperature in a way that ensured little overall change in net aggregation rate. The apparent aggregation rate in Figure 4A changed a few percent between 10 and 25 °C. In contrast, the viscosity of water decreases by about 31.5% in the same temperature interval. Divalent cation binding constants change very little in this temperature range (McLaughlin et al., 1981). Thus these data are consistent with the hypothesis that the rate of aggregation is controlled by the amount of bound divalent cation (see section 6a below).

Unlike liposome aggregation, the Ca^{2+}-induced lipid-mixing rates were extremely dependent on temperature. Little or no lipid mixing was observed at 10 °C (Figure 4B), which is close to the T_m of BBPS in the NaCl buffer (9 °C for this lot of BBPS). Although there was an increase in fluorescence at 10 °C in the example shown, this occurred after a considerable delay and corresponded to the later changes in the scatter curve, which probably represent subsequent rearrangement within large aggregates of liposomes, possibly into cochleate structures. This delay was also similar to the delay prior to leakage of the aqueous contents from similar liposomes under these conditions (data not shown). In contrast, the fluorescence vs time curves for systems at higher temperatures had steep initial slopes indicating that liposome destabilization occurs during the initial encounters between liposomes.

(4) DPX Effects on PS-Liposome Aggregation and Lipid-Mixing Rates

To determine whether the DPX effect of lowering T_m (Figure 1b,c) was correlated with altered interactions between liposomes, aggregation and lipid-mixing rates were compared between control and DPX-containing liposomes. Liposomes prepared with 90 mM DPX encapsulated had different time-dependent aggregation curves although it appears that the initial rates of aggregation were the same (Figure 5A). The difference in aggregation behavior may be a direct effect of the DPX on liposome–liposome affinity or may be a scatter-related artifact (i.e., different fractional increase in scatter/aggregate) consistent with their smaller average diameter (about 60 nm compared to 70 nm of the control liposomes). More strikingly, the DPX-containing liposomes exhibited lipid-mixing rates that were consistently larger than the rates for liposomes prepared in the standard NaCl buffer, and the difference in rates was greatest at lower temperatures (Figure 5, panel B vs panel C). Specifically, DPX increased the initial rates by factors of 12.8, 2.6, and 1.7 over control at 10, 20, and 30 °C, respectively. The difference in rate persisted when Ba^{2+} was substituted for Ca^{2+} as the divalent cation used to initiate lipid mixing (not shown). DPX had no effect on the threshold concentration of Ca^{2+} required for liposome aggregation or lipid mixing (not shown).

Since fusion rates are significantly faster when SUV are compared with LUV under otherwise identical conditions (Wilschut et al., 1980, 1981; Bentz & Duzgunes, 1985), we fractionated the two types of liposomes on a Sephacryl S1000 column and compared the behavior of identical size fractions at several lipid concentrations. The differences in aggregation behavior and lipid-mixing rates persisted. For both control and DPX-containing liposomes, there were no significant differences in aggregation or lipid-mixing kinetics between the size-fractionated populations suggesting that, in this range, size does not contribute significantly to either apparent rate.

(5) POPS Liposomes Do Not Exhibit Lipid Mixing

Aggregation and lipid-mixing rates were determined for POPS LUVs under conditions that were identical to those used with BBPS liposomes. Although POPS aggregated avidly when divalent cations were added, no lipid mixing was observed (Figure 6) at temperatures well above T_m (11.5 °C, Figure 1). Similar conclusions were obtained with ANTS–DPX contents-mixing experiments with up to 5 mM Ca^{2+} (not shown). The POPS and BBPS liposome sizes appeared identical by gel filtration chromatography and encapsulated volume comparisons. Therefore the only major difference between them is the composition and distribution of the acyl chains. Each molecule of POPS contains identical acyl chains, one saturated and one unsaturated. In contrast, BBPS is a natural product with mixed chains of variable length and degree of unsaturation. The principle fatty acids in BBPS are 18:0, 18:1, 20:1, 20:4, and 22:6, at about 41, 30, 2, 3, and 9%, respectively (product analysis by Avanti Polar Lipids, Inc.).

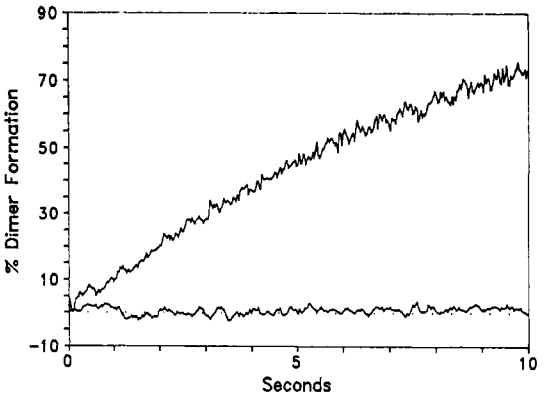

FIGURE 6: Lipid-mixing rate shown by the percent ideal dimer formation vs time for POPS LUVs (lower trace) compared with that for BBPS liposomes (upper trace) induced by 3 mM Ca^{2+} at 25 °C.

(6) Comparison of Ba^{2+}- and Ca^{2+}-Induced Aggregation and Lipid Mixing between BBPS Liposomes

Although there is significant evidence suggesting that not all divalent cations are equally effective as promoters of aggregation and fusion, the bases for these differences are not well understood (Wilschut et al., 1981; Bentz et al., 1983; Duzgunes et al., 1984; Bentz & Duzgunes, 1985). The next set of experiments was designed to reexamine both aggregation and lipid mixing in the Ca^{2+}– and Ba^{2+}–PS systems using the methods described in the previous sections that improve our ability to resolve the initial rates. We compared the temperature dependence of lipid mixing for these two divalent cations at concentrations of the ions that produce equal aggregation rates as a means of identifying differences in lipid defect formation rates.

(a) Aggregation and Lipid Mixing vs Divalent Cation Concentration. In agreement with others [reviewed in Nir (1991)], we found that the threshold concentrations for aggregation and lipid mixing between BBPS LUVs are approximately 1.5 mM for Ba^{2+} and 2.5 mM for Ca^{2+} at neutral pH. Both aggregation and lipid-mixing rates increased rapidly and nonlinearly with increasing divalent cation concentration above these thresholds (not shown). When compared at equal concentrations (e.g., 3 mM Ba^{2+} vs Ca^{2+}), the Ba^{2+}-induced aggregation rate was greater than the Ca^{2+}-induced rate over the entire temperature range that was examined (10–50 °C) (Figure 7) consistent with previous results for SUVs at 24 °C (Ohki et al., 1982).

To make a more detailed comparison of the effects of Ba^{2+} and Ca^{2+} on the postaggregation step in lipid mixing, we compared the rates of lipid mixing at concentrations of Ba^{2+}

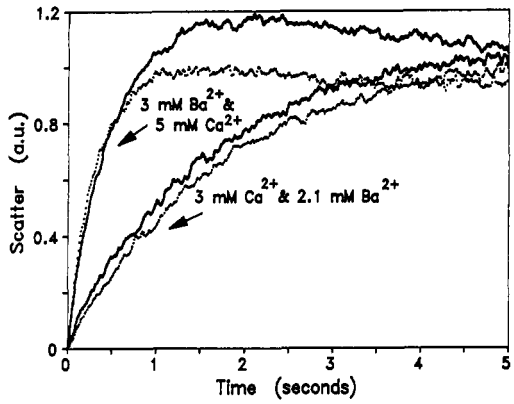

FIGURE 7: Aggregation rates as a function of the concentration and type of divalent cation. Examples of aggregation when the divalent cation concentrations are adjusted to give equivalent initial rise in scattered intensity subsequent to mixing. The upper traces are representative of the effect of 3 mM Ba^{2+} (solid line) and 5 mM Ca^{2+} (dashed line). The lower traces were obtained with 2.1 mM Ba^{2+} (solid line) and 3 mM Ca^{2+} (dashed line). When both divalent cations are at the same concentration (3 mM), the Ba^{2+}-induced aggregation rate is greater than that of Ca^{2+}.

and Ca^{2+} that yielded nearly the same rates of aggregation, as determined via light scattering. By trial and error, it was found that 2.1 mM Ba^{2+} induced aggregation rates nearly equal to those induced by 3.0 mM Ca^{2+} (a net aggregation rate of about 4.3×10^8 M^{-1} s^{-1}), and the effect of 3.0 mM Ba^{2+} was very similar to that of 5.0 mM Ca^{2+} (net aggregation rate of about 6.6×10^8 M^{-1} s^{-1}). Each of these pairs of Ba^{2+} and Ca^{2+} concentrations is nearly identical to the pair expected to yield equivalent degrees of saturation of the PS binding sites with the respective divalent cations, as judged from zeta potential determinations. According to McLaughlin et al. (1981), the zeta potential of BBPS is −24.8 mV when equilibrated with either 3 mM Ba^{2+} or 5 mM Ca^{2+}, and the zeta potentials for 2 mM Ba^{2+} and 3 mM Ca^{2+} are −29.7 and −28.9 mV, respectively. The interpolated value for 2.1 mM Ba^{2+}, the concentration we used, is −29.3 mV, quite close to the value for 3 mM Ca^{2+}. The near equivalence of the net aggregation rate induced by Ca^{2+} and Ba^{2+} under these two sets of conditions indicates that the surface charge density is the major determinant of this rate.

Although the initial segments of the scattering vs time curves at each pair of Ca^{2+} and Ba^{2+} concentrations were nearly identical (Figure 7), the long-time behaviors were different. It is not clear why this difference exists. For example, it could be due to differences in the average sizes or shapes of the larger aggregates in the two systems, differences in the disaggregation rates, or to different indices of refraction (hence light scattering power) of these two chemically different ion–lipid complexes.

(*b*) *Temperature Dependence of Lipid Mixing: Ca^{2+} vs Ba^{2+}.* Lipid-mixing rates were determined as a function of temperature for Ba^{2+} and Ca^{2+} combined with PS liposomes at two different concentrations of each divalent cation corresponding to conditions where the aggregation rates were identical. The rate of lipid mixing depended on the concentration and type of divalent cation as well as the temperature. First, lipid-mixing rates increased with increasing concentrations of Ca^{2+} or Ba^{2+} with a dependence similar to that for aggregation as has been shown previously (Wilschut et al., 1981; Bentz & Duzgunes, 1985). When lipid-mixing rates are compared under conditions where the aggregation rates and the extent of divalent cation binding are identical for Ba^{2+} and Ca^{2+} (2.1 mM Ba^{2+} and 3 mM Ca^{2+} or 3 mM Ba^{2+} and 5 mM Ca^{2+}), Ca^{2+}-induced lipid-mixing rates were greater than those with Ba^{2+} over most of the temperature range observed (the rates were nearly identical at 15 °C) despite the higher binding constant for Ba^{2+}. The lipid-mixing rate increased with temperature for both divalent cations (Figure 8a,b). However, the steepness of this dependence was substantially greater for the calcium than barium system (Figure 9). Specifically, from 10 to 50 °C, the Ca^{2+}-induced rates increased about 34-fold and those induced by Ba^{+2} rose closer to 10-fold. However, the lipid-mixing rate of Ba^{2+}–PS liposomes continued to increase with temperature well above 23.9 °C, T_m for the equilibrated Ba^{2+}–BBPS system (Figure 1d). Thus, as was noted previously for PS liposomes, T_m for the lipid–divalent cation complex was not absolutely correlated with fusion (Duzgunes et al., 1984; Bentz et al., 1985), i.e., the existence of the gel state patches of PS–divalent cation complex were not required for fusion to occur.

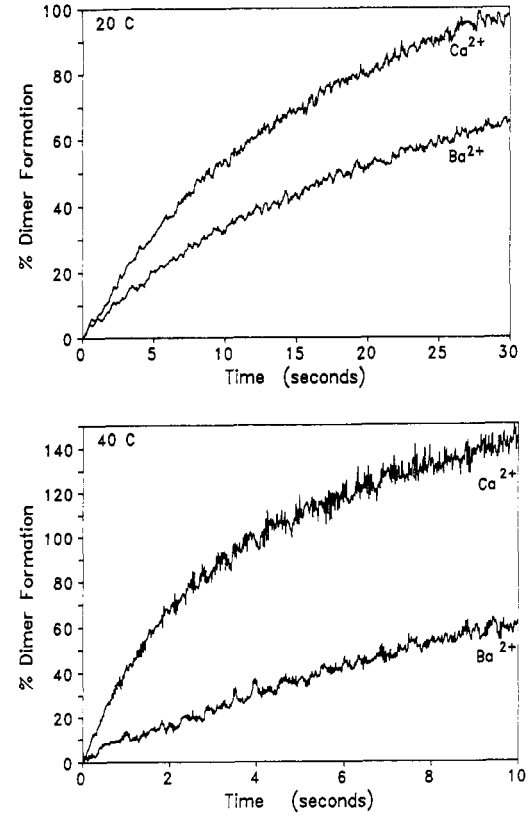

FIGURE 8: Lipid-mixing curves (percent dimer formation vs time) at 20 and 40 °C when the two divalent cations are at concentrations that give equal net aggregation rates. In all cases the aggregation rate is not rate-limiting. (a, top) The rise of F_{NBD}, corrected to indicate the percent of ideal fused dimer formation, associated with lipid mixing for BBPS liposomes (200 μM in BBPS) in 2.1 mM Ba^{2+} (lower trace) or 3 mM Ca^{2+} (upper trace) at 20 °C. (b, bottom) Lipid mixing as in panel a at 40 °C.

An Arrhenius plot of these data is shown in Figure 9B. Both sets of data (Ca^{2+} and Ba^{2+} ions) are essentially linear over the temperature range where the rates observed primarily represent the lipid defect formation step rather than aggregation. There was no apparent break in the Arrhenius plot for Ba^{2+}–BBPS lipid-mixing rates at or near T_m and thus no evidence from these studies that the molecular pathway for lipid mixing was significantly different above and below T_m. The slopes of the plots depended on the type and not the concentration of divalent cation (Table I). The intercepts, on the other hand, varied both with the type (Ba^{2+} vs Ca^{2+}) and concentration of divalent cation used.

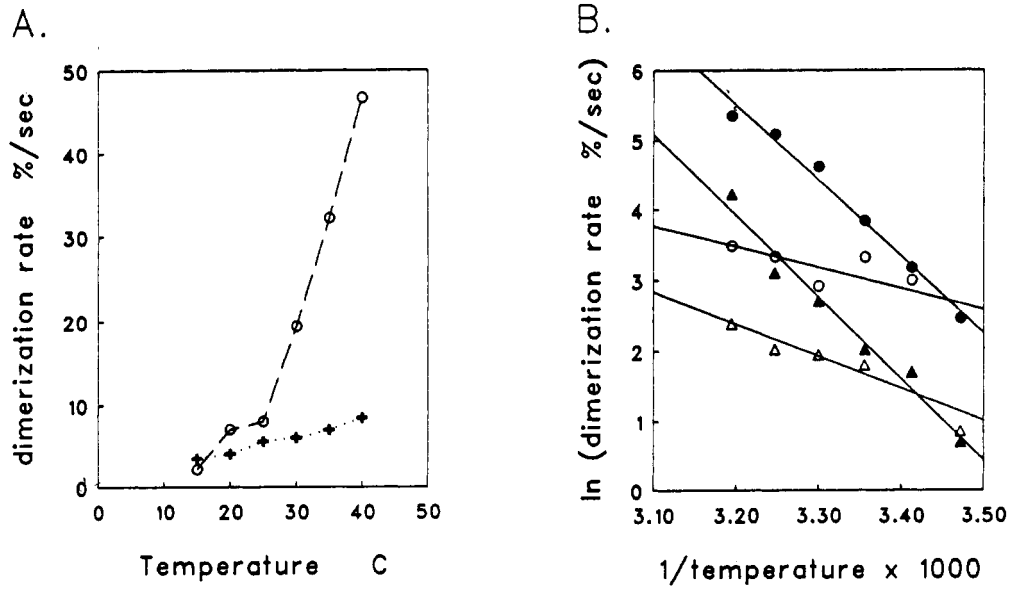

FIGURE 9: The temperature dependence of the Ba^{2+}- and Ca^{2+}-induced lipid mixing of BBPS liposomes. (A) The apparent initial rates of lipid mixing taken from the linear portion of plots, plotted as a function of temperature for liposome interactions induced by 2.1 mM Ba^{2+} (+) and 3 mM Ca^{2+} (O). The concentration of BBPS is 200 μM. (B) The ln of the rates of lipid mixing observed for 200 μM BBPS plotted as a function of $1/T$ when the divalent cation concentrations were 2.1 and 3 mM Ba^{2+} (open triangles and open circles, respectively) and for 3 and 5 mM Ca^{2+} (closed triangles and closed circles, respectively). The lines represent the least-squares linear fit to the data.

Table I: Slopes of the Arrhenius Plots of the Lipid-Mixing Rates for Ba^{2+}- and Ca^{2+}-Induced Events

	Ba^{2+}		Ca^{2+}	
[BBPS] (μM)	2.1 mM	3.0 mM	3.0 mM	5.0 mM
80		-5.7	-10.7	
160		-5.2	-12.6	
200	-4.6		-11.6	-10.9
200	-3.1		-10.7	
200		-4.9		-10.4

DISCUSSION

Previous studies of divalent cation-induced acidic lipid fusion have emphasized the difficulty of determining the rate constants for aggregation and defect formation (Bentz & Ellens, 1988; Duzgunes & Bentz, 1988; Nir, 1991). Here, we have applied stopped-flow mixing in an attempt to semi-quantitatively compared liposome aggregation and lipid-mixing defect formation rates under different circumstances, without application of a complex kinetic analysis of the data. The advantages of stopped-flow mixing make this possible within a limited yet important range of concentrations and temperatures. By studying the effects of system composition and temperature on these two rates, one can make inferences concerning the mechanism of the underlying processes. Specifically, we have used this approach to compare Ca^{2+}- and Ba^{2+}-induced BBPS liposome aggregation and lipid-mixing rates. Our conclusions are that the aggregation rates correlate with the percent of PS bound with divalent cation, that aggregation is relatively independent of temperature, and that the difference between lipid-mixing rates induced by these two divalent cations is reflected in very different temperature dependencies. In the course of developing the methods used in this study, we showed that the collisional quencher DPX perturbs PS in such a way as to increase lipid-mixing rates when encapsulated and to decrease T_m. Furthermore, PS with defined acyl chains is resistant to lipid mixing.

In these studies we have measured lipid-mixing rates rather than contents-mixing rates in order to avoid artifacts introduced by the contents measuring scheme itself. We feel that the lipid-mixing process we observe corresponds to a lipid defect formation (possibly fusion) for two reasons. First, the divalent cation thresholds and temperature dependence correlate well with previous hand-mixing experiments where fusion was assayed by contents mixing using Tb/DPA (Bentz et al., 1983, 1985; Duzgunes et al., 1984; Wilschut et al., 1985). Second, lipid mixing did not occur between aggregated liposomes at low temperatures, when Mg^{2+} was used to aggregate the liposomes, or when the lipid was POPS, even after long times (5–10 min). Thus, neither lipid mixing nor changes in energy transfer efficiency occur via incidental processes like probe exchange between two closely apposed bilayers on the time scale of these experiments (seconds). It is probable that probe exchange occurs via nonfusion processes at very long times (Figure 4B), but care was taken to avoid contributions from these sources. It is possible that these data represent a situation where only the contacting monolayers exhibit lipid mixing, and, for this reason, we caution the reader that the event measured may not be true fusion between liposomes.

(1) Stopped-Flow Mixing Is a Useful Tool for Studying Liposome Fusion. Although it has been appreciated for a long time that the half-times of membrane fusion are on the order of seconds or faster, very few investigators have applied stopped-flow techniques to studying the problem (Morris et al., 1979, 1985; Blumenthal et al., 1991). In this study we have shown that the stopped-flow technique can be used with liposomal systems and extends the concentration and temperature ranges accessible. Thus, some new quantitative questions can be addressed.

The net rate constants for aggregation are greater than those previously reported. With 3 mM Ca^{2+}, the value obtained in these studies was (3–4) $\times 10^8$ M^{-1} s^{-1}. With 5 mM Ca^{2+}, the rate constant for aggregation is about 6×10^8 M^{-1} s^{-1}. Both of these are nearly 10-fold greater than many previous estimates for comparable systems [compiled in Nir (1991)] but still 5–10-fold less than the rate expected if the system were completely diffusion limited, i.e., about 3×10^9 M^{-1} s^{-1} at 25 °C. One likely reason for these differences is the improved time resolution of the present studies.

We compared lipid-mixing rates by analyzing data only in the early stages of liposome–liposome interaction. Conditions for the reaction were identified for which the overall rate was dominated by the rate of lipid defect formation (although we recognize that these defect formation rates are slight underestimates of the true rates since there is always an aggregation rate contribution). We verified this for each experiment in two ways. First, the lipid concentration dependence was determined for lipid-mixing rates, and only those values in regimes where the overall reaction appeared to be first order were used. Second, the aggregation process was observed for each experiment by light scattering to give an independent estimate of the aggregation rate. The latter is not a new idea, but the observation that the initial rise in scattering for PS–divalent systems can be directly correlated with the formation of dimeric aggregates has rarely been recognized. The temperature dependence of lipid mixing could not have been determined without the stopped-flow data for a series of lipid concentrations at each temperature.

(*2*) *DPX Lowers T_m and Increases Lipid-Mixing Rates.* One result of this study is that 90 mM DPX, the concentration typical for contents-mixing assays for membrane fusion, both lowered the phase transition temperature for PS (Figure 1b,c) and increased the lipid-mixing rate when it was encapsulated in the liposomes (Figure 5B,C). Other more subtle changes are suggested by the observation that liposomes prepared with DPX were somewhat smaller than liposomes prepared in NaCl buffer. The fact that DPX can increase lipid-mixing rates might explain the differences in membrane fusion rates ascertained when comparing the two frequently used contents-mixing assays, ANTS–DPX and Tb–DPA (Duzgunes et al., 1987b), and underscores the importance of confirming that the components of the assay method do not perturb the system of interest.

The structure of DPX suggests that it could associate with negatively charged PS bilayers. DPX is a bivalent cation, with the two charges separated by about 0.72 nm, which is also approximately the spacing between adjacent PS headgroups at the lipid/water interface. DPX also has one xylene and two pyridinium rings, which may partially penetrate into the hydrophobic region of the bilayer, while the positively charged moieties associate with anionic PS headgroups. If DPX binds in this manner, the PS acyl chains would be partially disordered, which is consistent with DPX lowering the T_m by about 10 °C.

The ability of DPX to influence the lipid-mixing rate is particularly interesting because the DPX is encapsulated within the liposomes, where it should be accessible only to the inner monolayer lipids. DPX did not leak from the liposomes, nor is it likely that it remained bound to the PS outer membrane surface: the same results were obtained from liposomes several days after preparation and from liposomes that had been rechromatographed. The DPX effect may be an example of how modulating the transmonolayer properties may alter lipid-mixing rates, demonstrating that the rate-limiting steps in fusion include both destabilization of the apposed outer monolayers and the bilayer rearrangements required to complete the process. The observation that POPS liposomes undergo little or no lipid mixing is further indication that lipid defect formation rates for PS systems can be controlled by factors other than headgroup chemistry or T_m. An unanswered question is whether all perturbations that decrease T_m of the inner monolayer will also increase lipid-mixing rates in this system.

(*3*) *Relationship between Aggregation and Lipid-Mixing Rates of PS Liposomes to the Surface Potential of the Liposomes.* We show that PS vesicle aggregation rates correlate with the fraction of PS bound to divalent cation prior to the vesicle–vesicle contact. Temperature has little effect on aggregation rates or on the divalent cation binding constants (McLaughlin et al., 1981). Thus, over a range of conditions, initial aggregation rates are determined by the net surface charge of the liposomes.

Lipid-mixing rates increase as the percentage of PS bound to divalent cation increases (Wilschut et al., 1981; Bentz & Duzgunes, 1985), but the correlation between surface potential and lipid-mixing rates does not extend across the type of divalent cation or temperature. Specifically, although Ba^{2+} has a higher affinity for PS than does Ca^{2+}, when the rates of lipid mixing induced by the two ions are compared at equivalent PS binding site saturation, the Ca^{2+}-induced lipid-mixing rate is faster at or above 20 °C. Hauser and Shipley (1984) measured the spacing between dipalmitoyl-PS bilayers equilibrated with excess Ca^{2+} or Ba^{2+} and concluded that Ba^{2+} caused condensation in the plane of the bilayer but did not change the bilayer spacing, whereas Ca^{2+} condensed the lipids, induced a chain tilt, and decreased the interbilayer spacing. Preliminary ^2H NMR results suggest the acyl chain regions behave very differently when BBPS is equilibrated with Ba^{2+} as compared to Ca^{2+} (A. Walter, P. Yeagle, and D. P. Siegel, manuscript in preparation). How these differences relate to the differences in efficacy or mechanism of lipid mixing observed with these two divalent cations must await further study.

It is not clear whether ion binding to the surface of isolated bilayers [as in McLaughlin et al. (1981)] is the most relevant binding mode when considering fusogenicity or related processes. The binding constant for Ca^{2+} between two BBPS bilayers is significantly higher [$K_b = (1.4–4) \times 10^6$ M^{-1}] (Feigenson, 1986, 1989) than the value for a single bilayer ($K_b = 12$ M^{-1}) (McLaughlin et al., 1981). A comparable value for Ba^{2+}–PS has not been determined. Unfortunately, it is not obvious that the high-affinity binding is relevant for the measurements described here due to the relatively long times required for equilibration (Feigenson, 1986, 1989), nor is it known precisely where the divalent cation is bound during the lipid-mixing process. Although McLaughlin et al. (1981) assumed that the electrostatic interactions occur completely on one monolayer surface, when the liposomes come together the divalent cation is thought to form an electrostatic linkage between phosphate groups of the PS molecules on the apposed monolayers (Newton et al., 1978, Casal et al., 1987; Mattai et al., 1989).

(*4*) *Temperature Dependencies of Ba^{2+}- and Ca^{2+}-Induced Lipid-Mixing Rates.* The rate of Ba^{2+}-induced lipid mixing increased with temperature and the temperature dependence was linear in an Arrhenius-type plot over the entire temperature range tested (10–40 °C) (Figure 9B). This result indicates that patches of frozen bilayer are neither required nor appear to affect the lipid destabilization process in the divalent cation–PS system.

The rate of lipid mixing induced by Ca^{2+} also increased with temperature, and the Arrhenius-type plots were linear (Figure 9). However, the slopes of the plots for the Ca^{2+} data are more than twice as large as the slopes for the Ba^{2+} data. These data indicate that despite the fact that the Ca^{2+}-induced rates are faster at or above 20 °C when the fractional PS binding is the same, the apparent activation enthalpy of one or more postaggregation steps in the Ca^{2+}-induced lipid mixing

is larger than for the Ba^{2+}-induced process. The Ca^{2+}-induced rates could be faster at each temperature because the entropies of activation or the attempt frequencies (or both) are larger for the Ca^{2+}- as opposed to the Ba^{2+}-induced lipid mixing. Moreover, the slopes, but not the intercepts, of Arrhenius plots for both concentrations of Ca^{2+} and both concentrations of Ba^{2+} were similar (Figure 9B, Table I). Thus, for lipid mixing, the apparent enthalpy of activation seems to be relatively independent of the fraction of PS bound to divalent cation. The increase in rate with increasing divalent cation concentration therefore could be due to a change in the entropy of activation, or, more likely, due to either a change in the number of potential defect-forming sites between each pair of liposomes or an increase in attempt frequency per site.

Together these data suggest that there are qualitative differences between the mechanisms of lipid mixing induced by these two ions. These mechanistic differences may be related to the differences in divalent cation–PS complex structure as noted above (Hauser & Shipley, 1984) or the surface hydrophobicity induced by each of these ions (Ohki & Arnold, 1990). These data, in combination with the results with DPX and POPS, imply that there are several contributing factors determining the rate of lipid-defect formation and that these can be altered independently.

Conclusions. Stopped-flow mixing permits data acquisition in time regimes that permit more reliable measurements of liposome aggregation and over a wider temperature and lipid concentration range than has been accessible previously. By using this technique, it is possible to estimate the lipid-mixing rates directly from the initial overall rates, rather than fitting the data to derive the aggregation and fusion rate constants. Although many of the conclusions made previously by other methods were substantiated in this study, application of these methods revealed that aggregation rates in divalent cation–BPPS systems are greater than previously estimated. Comparison of the temperature dependencies of Ba^{2+}- and Ca^{2+}-induced lipid mixing showed that the apparent overall activation enthalpy is greater for Ca^{2+} than for Ba^{2+}, that the enthalpic term does not vary with moderate changes in divalent cation concentration, and that the difference in lipid-mixing rates as a function of divalent cation concentration may lie in the overall entropy of activation or in the attempt frequency. The physical meaning of these results remains to be ascertained. The more peripheral aspects of these studies, i.e., the effect of encapsulated DPX and inability of POPS to undergo lipid mixing, indicate that the characteristics of the trans-monolayer and of the acyl chain region are likely to be significant determinants of the overall rate of lipid mixing. Identifying the key aspects of these parameters will surely help define both the path and energetic limits to membrane fusion events.

ACKNOWLEDGMENT

We are very grateful to the meticulous assistance given by Ms. Debbie Clark and Ms. Dianne Dewey, who have had essential roles in carrying out the aggregation and lipid-mixing experiments. In addition, we greatly appreciate the efforts of Ms. Nancy Reeder and Mr. James C. Banschbach, who obtained most of the DSC data. We thank Ms. Gloria Story and Dr. Curtis Marcott for aid in acquiring and interpreting the FTIR spectra and Dr. Peter Lauf for the use of his chloride titrator. Mr. Habib Khan's help during manuscript preparation is most appreciated.

REFERENCES

Almers, W., & Tse, F. W. (1990) *Neuron 4*, 813–818.

Ames, B. N., & Dubin, D. T. (1960) *J. Biol. Chem. 235*, 769–775.

Bentz, J., & Duzgunes, N. (1985) *Biochemistry 24*, 5436–5443.

Bentz, J., & Ellens, H. (1988) *Colloids Surf. 30*, 65–112.

Bentz, J., Duzgunes, N., & Nir, S. (1983) *Biochemistry 22*, 3320–3330.

Bentz, J., Duzgunes, N., & Nir, S. (1985) *Biochemistry 24*, 1064–1072.

Blumenthal, R. (1987) *Curr. Top. Membr. Transp. 29*, 203–254.

Blumenthal, R., Schoch, C., Puri, A., & Clague, M. J. (1991) Calcium entry and action at the presynaptic terminal, *Ann. N.Y. Acad. Sci. 635*, 285–296.

Casal, H. L., Martin, A., Mantsch, H. H., Paltauf, F., & Hauser, H. (1987) *Biochemistry 26*, 7395–7401.

Duzgunes, N., & Bentz, J. (1988) in *Spectroscopic Membrane Probes* (Loew, L. M., Ed.) Chapter 6, pp 117–159, CRC Press, Boca Raton, FL.

Duzgunes, N., Paiement, J., Freeman, K. B., Lopez, N. G., Wilschut, J., & Papahadjopoulos, D. (1984) *Biochemistry 23*, 3486–3494.

Duzgunes, N., Allen, T. M., Fedor, J., & Papahadjopoulos, D. (1987) *Biochemistry 26*, 8435–8442.

Ellens, H., Bentz, J., & Szoka, F. (1985) *Biochemistry 24*, 3099–3106.

Ellens, H., Siegel, D. P., Alford, D., Yeagle, P. L., Boni, L., Lis, L. J., Quinn, P. J., & Bentz, J. (1989) *Biochemistry 28*, 3692–3703.

Feigenson, G. W. (1986) *Biochemistry 25*, 5819–5825.

Feigenson, G. W. (1989) *Biochemistry 28*, 1270–1278.

Fung, B. K.-K., & Stryer, L. (1978) *Biochemistry 17*, 5241–5248.

Hauser, H., & Shipley, G. G. (1984) *Biochemistry 23*, 34–41.

Hope, M. J., Bally, M. B., Webb, G., & Cullis, P. R. (1985) *Biochim. Biophys. Acta 812*, 55–65.

Mattai, J., Hauser, H., Demel, R. A., & Shipley, G. G. (1989) *Biochemistry 28*, 2322–2330.

McLaughlin, S., Mulrine, N., Gresalfi, T., Vaio, G., & McLaughlin, A. (1981) *J. Gen. Physiol. 22*, 445–473.

Morris, S. J., Hellweg, M. A., & Haynes, D. H. (1979) *Biochim. Biophys. Acta 553*, 342–350.

Morris, S. J., Gibson, C. C., Smith, P. D., Strik, C. W., Bradley, D., Haynes, D. H., & Blumenthal, R. (1985) *J. Biol. Chem. 260*, 4122–4127.

Newton, C., Pangborn, W., Nir, S., & Papahadjopoulos, D. (1978) *Biochim. Biophys. Acta 506*, 281–287.

Nir, S. (1991) in *Membrane Fusion* (Wilschut, J., & Hoekstra, D., Eds.) Chapter 5, pp 127–153, Marcel Dekker, Inc., New York.

Nir, S., Duzgunes, N., & Bentz, J. (1983) *Biochim. Biophys. Acta 735*, 160–172.

Ohki, S., & Arnold, K. (1990) *J. Membr. Biol. 114*, 195–203.

Ohki, S., Duzgunes, N., & Leonards, K. (1982) *Biochemistry 21*, 2127–2133.

Ollivon, M., Walter, A., & Blumenthal, R. (1986) *Anal. Biochem. 152*, 262–274.

Papahadjopoulos, D. (1978) in *Membrane Fusion* (Poste, G., & Nicholson, G. L., Eds.) pp 765–790, Elsevier Press, New York.

Papahadjopoulos, D., Vail, W. J., Newton, C., Nir, S., Jacobson, K., Poste, G., & Lazo, R. (1977) *Biochim. Biophys. Acta 465*, 579–598.

Walter, A., Banschbach, J. L., & Siegel, D. P. (1991) *Biophys. J. 59*, 128a.

Wilschut, J., Duzgunes, N., Fraley, R., & Papahadjopoulos, D. (1980) *Biochemistry 19*, 6011–6021.

Wilschut, J., Duzgunes, N., & Papahadjopoulos, D. (1981) *Biochemistry 20*, 3127–3133.

Wilschut, J., Duzgunes, N., Hoekstra, D., & Papahadjopoulos, D. (1985) *Biochemistry* 24, 8–14.